MEDICAL SCIENCE MONITOR

ANIMAL STUDY

e-ISSN 1643-3750
© Med Sci Monit, 2019; 25: 9028-9041
DOI: 10.12659/MSM.917925

Received: 2019.06.04
Accepted: 2019.08.19
Published: 2019.11.28

Integrative Analysis of Expression Profiles of MicroRNAs and mRNAs in Treatment of Acute Myocardial Infarction with Compound Longmaining Decoction

Authors' Contribution:
Study Design A
Data Collection B
Statistical Analysis C
Data Interpretation D
Manuscript Preparation E
Literature Search F
Funds Collection G

BCE 1 Diaodiao Bu
BEF 2 Zhuo Su
BD 1 Mei Meng
AG 1 Changli Wang

1 College of Pharmacy, Shaanxi University of Chinese Medicine, Xianyang, Shaanxi, P.R. China
2 College of Pharmacy, Xi'an Jiao Tong University, Xi'an, Shaanxi, P.R. China

Corresponding Author: Changli Wang, e-mail: wcl3433@163.com
Source of support: This research work was supported by the National Natural Science Foundation of China (grant no. 81373944)

Background: This study identified microRNAs (miRNAs) and mRNAs associated with Compound Longmaining (CLMN) treatment of acute myocardial infarction (AMI). Our results provide a theoretical framework to guide AMI treatment and improve myocardial injury.

Material/Methods: The myocardial tissues of the sham operation group (S), the model group (M), and the CLMN treatment group (T) were obtained. The mRNA and miRNA expression profiles were identified using RNA-sequencing analysis. The sequencing results were verified by quantitative real-time PCR (qRT-PCR). Bioinformatics was used to predict the function of differentially expressed genes (DEGs) and related signal transduction pathways. The target genes of miRNAs were predicted by software analysis, and the relationship between miRNA and mRNA was studied by network analysis.

Results: RNA-sequencing revealed 22 differentially expressed miRNAs (DEMs) and 76 DEGs in myocardial tissue. Six DEMs and 9 DEGs were randomly selected for qRT-PCR validation, and corroborating results were obtained. The results of Gene ontology (GO) showed that DEGs participated in different biological processes. Through the combined analysis of miRNAs and mRNAs expression, it was confirmed that a single miRNA is involved in the regulation of multiple genes, and also multiple miRNAs can target one gene.

Conclusions: The analysis based on the miRNA-mRNA network can not only help to elucidate the potential molecular mechanism of CLMN treatment of AMI, but can also help in identifying novel therapeutic targets.

MeSH Keywords: MicroRNAs • Myocardial Infarction • Real-Time Polymerase Chain Reaction

Full-text PDF: https://www.medscimonit.com/abstract/index/idArt/917925

Indexed in: [Current Contents/Clinical Medicine] [SCI Expanded] [ISI Alerting System] [ISI Journals Master List] [Index Medicus/MEDLINE] [EMBASE/Excerpta Medica] [Chemical Abstracts/CAS]

Background

Coronary or ischemic heart disease is the result of coronary arterial atherosclerosis. The lesions caused by stenosis or obstruction can lead to ischemia, hypoxia, or necrosis. Acute myocardial infarction (AMI) is a more serious variant of coronary heart disease. AMI is a major cardiovascular disease that can seriously endanger human health worldwide. It has become one of the leading causes of death and disability in recent years [1]. It can induce myocardial cell remodeling, apoptosis, hypertrophy, fibrosis, and, ultimately, heart failure [2].

The prescription of Compound Longmaining (CLMN) for the treatment of coronary heart diseases was established and validated in the clinic by Professor Gen-yu Tao (Affiliated Hospital of Shaanxi University of Traditional Chinese Medicine). It consists of 4 traditional Chinese medicines (*Puerariae lobatae radix, Dioscoreae nipponicae rhizoma, Chuanxiong rhizoma,* and *Propolis*). Previous clinical studies have proved its efficacy for the treatment of AMI [3]. However, the specific mechanism of action of this formulation is still unclear. Therefore, it is important to explore the mechanism of action with respect to coronary heart disease.

Recently, many studies have been performed to understand AMI at the gene level. It is considered to be an extremely complex physiological and pathological process. The occurrence and development of AMI is a multilevel regulatory process happening at DNA, transcription, post-transcription, and protein expression levels. MicroRNAs (miRNAs) are endogenous regulatory RNA molecules that play an important role in the pathogenesis of AMI. They participate in a complex network of gene regulation through post-transcriptional negative regulation of the target RNA molecules and also in various pathophysiological processes with AMI and associated complications [4,5]. This effect of miRNAs on mRNA is well-known with respect to different physiological processes such as development, immunity, and neuronal activity [6]. Much evidence has also confirmed that small RNA-mediated RNA also regulates various diseases [7,8]. Valuable information can be obtained regarding the mechanism of CLMN action on AMI by a detailed understanding of the expression profiles of the related mRNAs and miRNAs.

The present study used high-throughput sequencing techniques to assess expression profiles of miRNAs and mRNA in response to CLMN treatment of AMI. We assessed the correlation among differentially expressed microRNAs (DEMs) and genes (DEGs), and explored the regulatory role of mRNA and miRNAs to identify novel therapeutic targets.

Material and Methods

Animals

A total of 18 male BALB/c mice, weighing 22–28 g, were purchased from the Animal Center of the Fourth Military Medical University (Shaanxi, China). The mice were allowed to acclimatize by keeping them under controlled humidity and temperature for 7 days. The protocol was approved by the Animal Ethics Committee of Shaanxi University of Chinese Medicine (Shaanxi, China).

Preparation of CLMN decoction

The CLMN decoction was prepared following a previously reported method [9]. Briefly, 48 g of each of the 4 traditional Chinese medicines were decocted in water (1: 14, w/v) twice, followed by condensation of the combined solution to 0.32 g/ml crude drug.

Model preparation and drug administration

All the animals were divided into 3 groups. The AMI model was established following a previously reported method [10,11]. Briefly, the process included opening the pericardium and visualizing the left anterior descending coronary artery. A needle was inserted and the artery was ligated with 8/0 monofilament polypropylene suture 2 mm from the lower edge of the left atrial appendage, leading to permanent ischemia of the coronary artery below the ligation line. In the sham operation group, needles were inserted into the left anterior descending branch of the coronary artery after thoracotomy, but they were not ligated, and the other operation procedures were similar to those used in the AMI model group. The animals in both the sham and model groups were given normal saline. The CLMN group was given CLMN decoction (6.24 g/kg/day). Mice were observed for 3 weeks.

Sample collection

After 21 days of intragastric administration, mice were anesthetized and fresh heart specimens were collected. Each sample was divided into 2 parts for pathology and miRNA-seq, mRNA-seq analysis, and qPCR.

Histological analysis

The myocardial tissues were fixed in 10% neutral formaldehyde solution for 24 h, then they were embedded, sliced, and stained with hematoxylin-eosin (HE) and Masson Trichrome. All samples were examined using an optical microscope (Olympus Optical Co., Tokyo, Japan). Image Pro-Plus 6.0 (IPP 6.0) image processing software was used to calculate the percentage of

Indexed in: [Current Contents/Clinical Medicine] [SCI Expanded] [ISI Alerting System] [ISI Journals Master List] [Index Medicus/MEDLINE] [EMBASE/Excerpta Medica] [Chemical Abstracts/CAS]

Table 1. qPCR reaction procedure.

Step	Temperature (°C)	Time	Number of cycles
Initial denaturation	95	10 min	1
Denaturation	95	15 s	
Annealing	60	30 s	40
Extension	72	15 s	
	95	15 s	
Dissociation	60	1 min	1
	95	15 s	

MI area (Infarction area percentage=myocardial infarction area/left ventricular total area) in each group.

Small RNA sequencing

Total RNA was extracted from the myocardial tissues using Trizol (Invitrogen). The RNA molecules 18–30 nucleotides in size were enriched by polyacrylamide gel electrophoresis (PAGE). The 3'adapters were added and the 36–44 nucleotide long RNAs were enriched. The 5'adapters were also ligated to the RNAs. The reverse transcription products were separated by 3.5% agarose gel electrophoresis. We selected the 140–160 bp zone strip for cutting glue, and the gel recovery product is the final library. Illumina HiSeqTM 2500 was sequenced by Gene Denovo Biotechnology Co. (Guangzhou, China). DEMs was screened by P value (<0.05) and fold change (≥1.5).

mRNA sequencing

RNA was extracted using Trizol (Invitrogen). Magnetic beads with Oligo (dT) were used to enrich the mRNA and to add fragmentation buffer to the obtained mRNA to make the fragment become a short fragment, and then the first strand of cDNA was synthesized by six-base random primer (random hexamers) using the mRNA as the template. The second strand of cDNA was synthesized by adding buffer, dNTPs, RNase H, and DNA polymerase I. The second strand of cDNA was purified by QiaQuick PCR kit and eluted with EB buffer. The end was repaired, base A was added, a sequencing junction was added, and then the target fragment was recovered by agarose gel electrophoresis. PCR amplification was carried out to complete the preparation of the whole library. The constructed library was sequenced with Illumina HiSeqTM 2500. DESeq software was used to identify DEGs in pair-wise comparisons with fold change (FC) ≥1.5 and false discovery rate (FDR) ≤0.25 [12,13].

Quantitative real-time PCR validation

To validate the expression profiles of the 6 miRNAs and 9 mRNAs obtained by miRNA-Seq and mRNA-Seq, qRT-PCR was performed using U6 and β-actin as references. The results were calculated using the comparative Ct ($2^{-\Delta\Delta}$Ct) method [14]. The qPCR reaction procedure is shown in Table 1. The qPCR primer sequences are shown in Supplementary Tables 1 and 2.

Prediction of miRNA-targeted genes and construction of miRNA-mRNA network

The DEMs were used to identify potential target genes by searching the RNAhybrid (v2.1.2) +svm light (v6.01), Miranda (v3.3a), and TargetScan (Version: 7.0) software. The data providing details about the intersection of DEMs target genes and DEGs were obtained. Cytoscape 3.6.1 software was used for network construction of miRNA-mRNA interaction.

GO Analysis and KEGG Pathway Analysis

The DEGs were input into Blast2GO (*https://www.blast2go.com/*) and Blastall (*http://www.kegg.jp/*) software for Gene Ontology (GO) analysis and Kyoto Encyclopedias of Genes and Genomes (KEGG) pathway enrichment analysis, respectively.

Statistical analysis

All results are expressed as mean±standard deviation. One-way ANOVA was used to compare the results of multiple groups. All statistical analysis was carried out by SPSS 19.0 software. P value less than 0.05 indicates that there was a statistically significant difference.

Results

Effect of CLMN on pathological changes

Masson trichrome staining results (Figure 1B, 1D) shown that the myocardial cells in S group were neatly arranged and clearly structured, with no proliferation of fibroblasts. The M group revealed an obvious myocardial interstitial collagen deposition along with severe myocardial fibrosis. As compared to the

Indexed in: [Current Contents/Clinical Medicine] [SCI Expanded] [ISI Alerting System] [ISI Journals Master List] [Index Medicus/MEDLINE] [EMBASE/Excerpta Medica] [Chemical Abstracts/CAS]

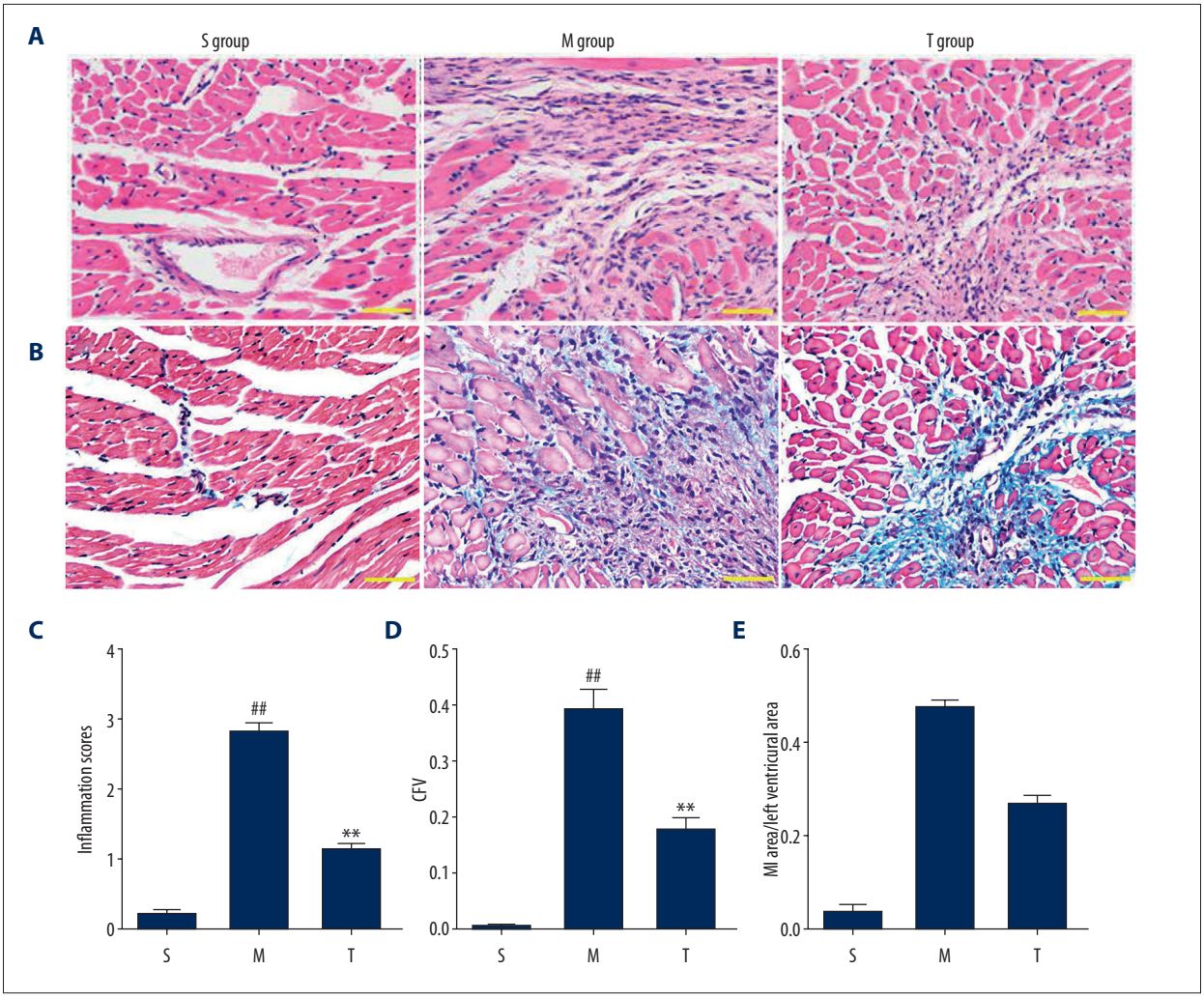

Figure 1. HE staining and Masson staining were used to detect the effect of CLMN on cardiac histopathological changes in mice. Representative sections (magnification: 400×). (**A**) HE staining. (**B**) Masson staining. (**C**) Inflammation scores of HE staining. (**D**) Collagen volume fraction (=Collagen-positive blue area/Total tissue area). (**E**) Percentage of MI area in each group of rats (Percentage of infarction area=MI area/Left ventricular area).

M group, significant reduction in the proliferation of cardiac fibroblasts and in myocardial interstitial fibrosis was observed in the T group. The HE staining suggests (Figure 1A, 1C) that the myocardial cells in the S group had clear cross-striation, uniform staining, and orderly arrangement. However, the myocardial tissue in the M group was seriously damaged, had uneven staining, blurred cross-striation, disordered arrangement, a large amount of cellular infiltration, and flaky necrosis, and the cell nuclei were smaller. Overall, the inflammatory symptoms were found to be largely alleviated in the T group. According to Figure 1E, the area of MI significantly decreased after the treatment of CLMN.

Identification of DEGs and DEMs

As shown in Figure 2B with respect to the S groups, a total of 1811 genes (632 up- and 1179 down-regulated) and 139 miRNAs (61 up- and 78 down-regulated DEMs) were differentially expressed in the M group. There were 175 DEGs (81 up and 94 down-regulated) and 56 DEMs (23 up- and 33 down-regulated) in the T group (Figure 3B). To further visualize the differences in the gene and miRNA expression profiles among these groups, a Venn map (Figures 2C, 3C) and heat map (Figures 2A, 3A) were created using RNA-seq and miRNA-seq data, showing that CLMN decoction regulates 76 DEGs (15 up- and 61 down-regulated) and 22 DEMs (11 up- and 11 down-regulated) in AMI. miRNA sequencing results are shown in Supplementary Table 3. In the mRNA sequencing, the number

Indexed in: [Current Contents/Clinical Medicine] [SCI Expanded] [ISI Alerting System] [ISI Journals Master List] [Index Medicus/MEDLINE] [EMBASE/Excerpta Medica] [Chemical Abstracts/CAS]

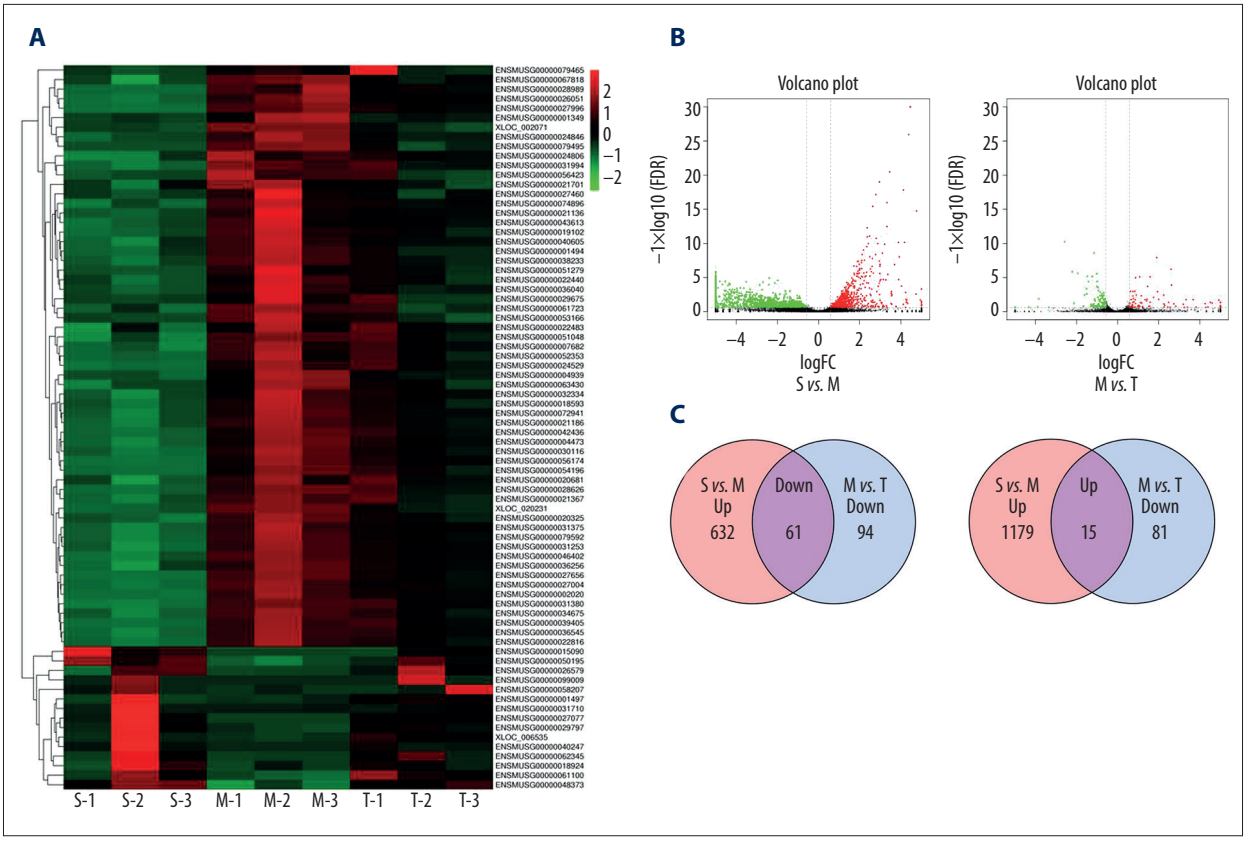

Figure 2. Screening for differential mRNA expresion. (**A**) Heat map of the differential mRNA expression. (**B**) Volcanic map of the differential mRNA expression. (**C**) Venn diagram of the differenial mRNA expression.

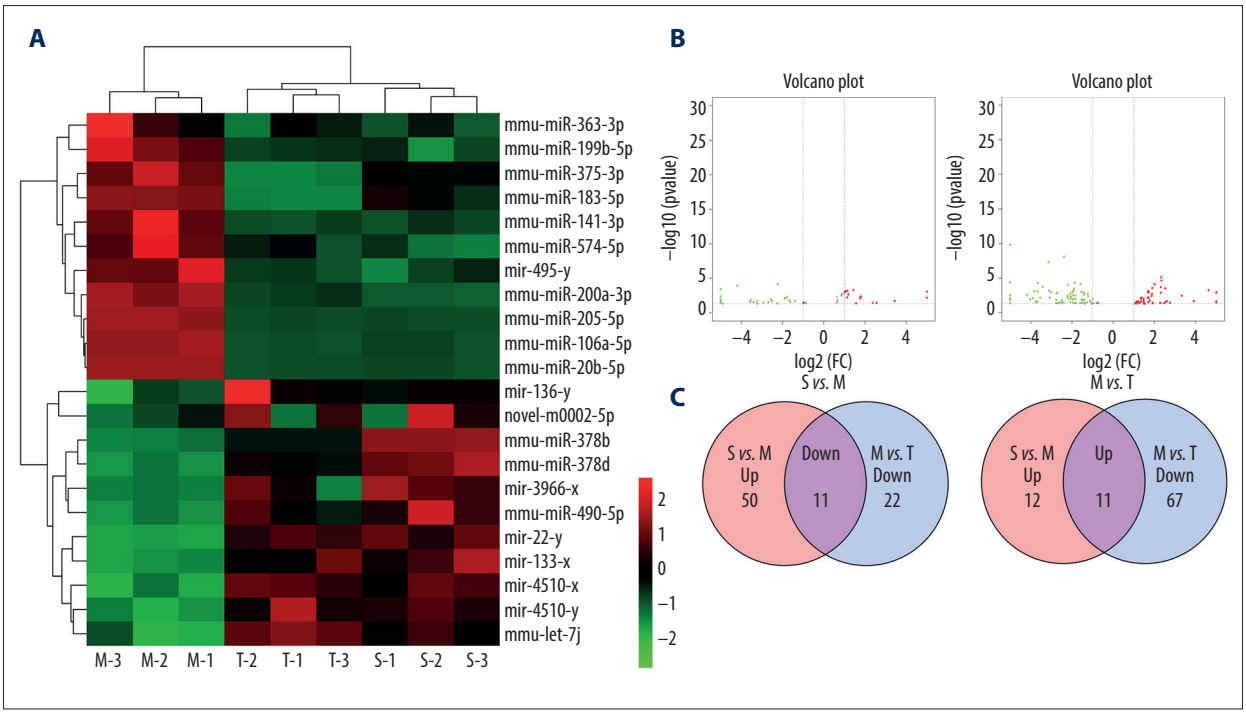

Figure 3. Screening for differential miRNA expression. (**A**) Heat map of the differential miRNA expression. (**B**) Volcanic map of the differenial miRNA expression. (**C**) Venn diagram of the differential miRNA expression.

Indexed in: [Current Contents/Clinical Medicine] [SCI Expanded] [ISI Alerting System] [ISI Journals Master List] [Index Medicus/MEDLINE] [EMBASE/Excerpta Medica] [Chemical Abstracts/CAS]

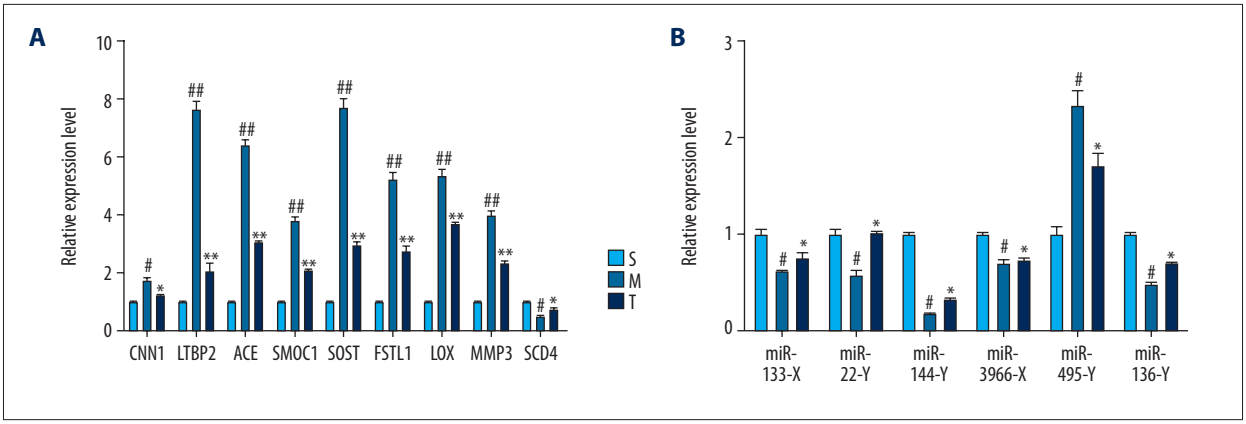

Figure 4. QPCR verification of DEGs and DEMs. (**A**) Q-PCR verification of selected DEGs. The relative expression levels of these genes were normalized to β-actin. (**B**) The relative expression of 6 DEMs determined by quantitative real-time PCR (qRT-PCR) analysis. The relative expression levels of miRNAs were normalized to U6 RNA. (# Significantly different from the S group ($p<0.05$); * Significantly different from the M group ($p<0.05$). ## Significantly different from the S group ($p<0.01$); ** Significantly different from the M group ($p<0.01$).

of reads in each sample was also calculated (Supplementary Table 4).

Validation of the sequencing data by quantitative RT-PCR

Quantitative RT-PCR (QRT-PCR) was used to verify the accuracy of transcriptome sequencing results. A total of 9 DEGs and 6 DEMs were selected based upon RNA-Seq and miRNA-seq data. These included CNN1, LTBP2, ACE, SMOC1, SOST, FSTL1, LOX, MMP-3, SCD4, mir-22-y, mir-495-y, mir-133-x, mir-144-y, mir-136-y, and mir-3966-x. Findings of QRT-PCR were corroborated by RNA-seq and miRNA-seq results (Figure 4).

GO analysis and KEGG pathway enrichment analysis were performed for DEGs

In order to elucidate the correlation between the DEGs and effects of the CLMN treatment on AMI, GO and signal pathway analysis were performed. Findings of the GO analysis showed that 61 down-regulated genes have different biological functions involved in regulation, single-organism process, cellular process, binding, and catalytic activity (Figure 5, Supplementary Table 5). KEGG signaling pathway analysis demonstrated that 76 DEGs were distributed in the 42 pathways, including Arachidonic acid metabolism, protein digestion and absorption, focal adhesion, ECM-receptor interaction, PI3K/Akt-, PPAR-, and TNF-signaling pathway (Figure 6, Supplementary Table 6).

Target prediction and construction of a regulatory and interaction network

A total of 8004 target genes were obtained from RNAhybrid (v2.1.2) +svm_light (v6.01) software, Miranda (v3.3a), and TargetScan (Version: 7.0) for 22 DEMs (Supplementary Table 7). We screened 76 DEGs by RNA-seq. Numerous studies have confirmed that miRNAs can regulate the degradation of RNA or inhibit its translation. Therefore, the expression level of miRNAs should be contrary to that of their target genes. Using this regulation mechanism, we intersected the transcriptome differential gene pool and the target gene pool of the difference obtained by the sequencing of miRNAs and found the overlapping genes of the 2 pools. Then, we determined the down-regulated differential target genes according to the up-regulation of miRNAs and up-regulated differential target genes by down-regulation of miRNAs. Relevance analysis showed that 9 of the 22 miRNAs were associated with differentially targeted genes, of which 8 were up-regulated (mir-3966-x, mir-4510-x, novel-m0002-5p, mir-144-y, mir-378d, mir-136-y, mir-22-y, and mir-133-x), and 1 was down-regulated (mir-495-y). However, because of the one-to-many, many-to-one relationship between miRNAs and RNA targeting regulation, single miRNAs can target multiple genes, and multiple miRNAs can target one gene. Therefore, not every gene targeted by up-regulated miRNAs is under-expressed, and every gene targeted by down-regulated miRNAs is over-expressed. Ultimately, we found 18 down-regulated genes (CST6, BACE2, WSCD2, FSTL1, P4HA3, CDH22, LTBP2, GM14296, DBN1, SOST, SRPX2, COL8A2, SMOC1, LOX, CNN1, COL4A3, ADAMTS8, and GDF6), and 2 up-regulated genes (SCD4 and PAX9). We then constructed a miRNA-gene interaction network based on the correlation between DEMs and DEGs expression (Figure 7).

Discussion

AMI is a serious and life-threatening cardiovascular disease that is associated with high morbidity, disability, and mortality.

Indexed in: [Current Contents/Clinical Medicine] [SCI Expanded] [ISI Alerting System] [ISI Journals Master List] [Index Medicus/MEDLINE] [EMBASE/Excerpta Medica] [Chemical Abstracts/CAS]

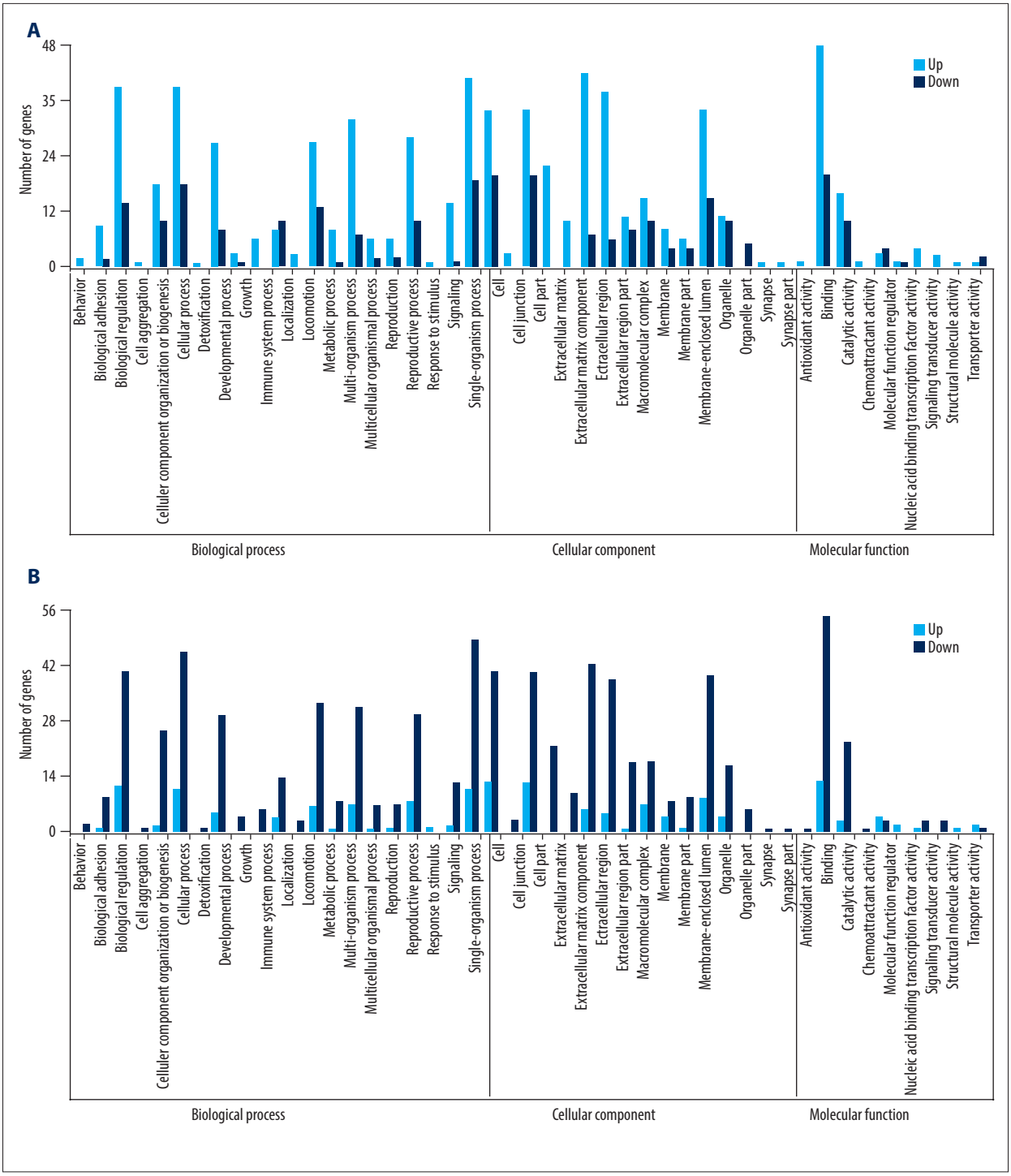

Figure 5. (**A**) S *vs.* M; (**B**) M *vs.* T. Gene ontology analysis of DEGs.

AMI is considered not only a common clinical emergency but also a public health problem that can endanger human health [15] and it is imperative to find an effective treatment for AMI. Previous studies have found that CLMN has protective effects on acute myocardial ischemia-hypoxia injury. In rats, it has been shown to resist thrombosis, improve microcirculation, and has protective effects on AMI [16]. In this study, we first used sequencing technology to screen DEMs and DEGs involved in the treatment of AMI. Finally, the differentiated miRNAs-mRNA regulatory network was constructed. Our findings have great relevance in deciphering the molecular mechanism associated with CLMN treatment of AMI.

Indexed in: [Current Contents/Clinical Medicine] [SCI Expanded] [ISI Alerting System] [ISI Journals Master List] [Index Medicus/MEDLINE] [EMBASE/Excerpta Medica] [Chemical Abstracts/CAS]

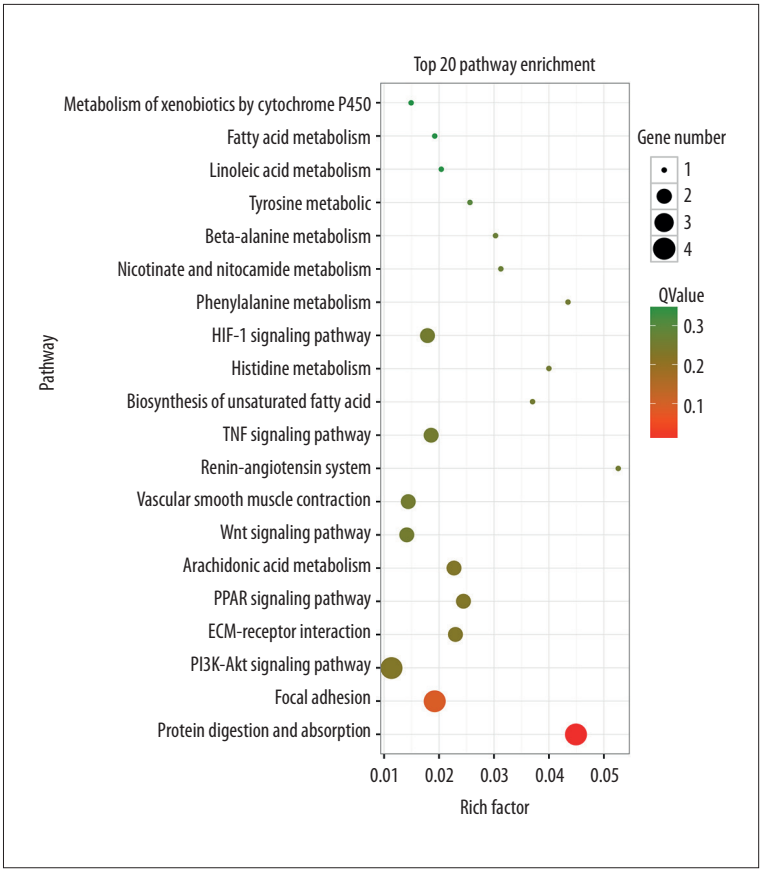

Figure 6. KEGG pathway analysis of DEGs (top 20).

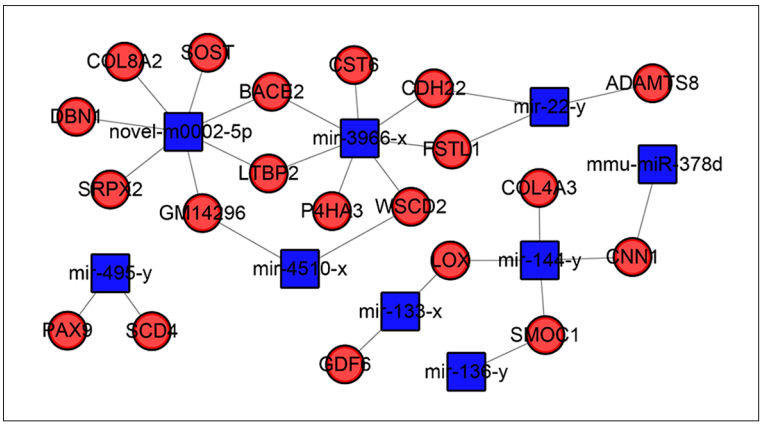

Figure 7. The miRNA-mRNA network diagram. The circle represents mRNA, the shape of the square represents miRNA, and their relationship is represented by a grey edge.

A total of 76 DEGs were obtained in this study. GO functional analysis of DEGs suggests these were mainly involved in biological regulation, single-organism process, cellular process, binding, catalytic activity, and extracellular region. The KEGG analysis revealed that the most significant enrichment pathways related to AMI were focal adhesion [17], PI3K-Akt signaling pathway [18], PPAR signaling pathway [19], ECM-receptor interaction [20], Arachidonic acid metabolism [21], and TNF signaling pathway [22]. Overall, this analysis suggests that the treatment of AMI by CLMN may operate through a variety of cellular responses and multiple pathways.

The development of AMI is a complicated process that may be regulated by multiple genes. In recent years, research interest in miRNAs has grown. In this study, 22 DEMs were selected, among which some miRNAs have been reported to play a role in AMI. Studies have demonstrated that mir-22 can prevent myocardial oxidative stress and can regulate cardiac apoptosis, hypertrophy, fibrosis, and regeneration [23–26]. mir-378 can inhibit the MAPK signal transduction pathway and control myocardial hypertrophy by acting on MAPK1, insulin-like growth factor-1 receptor, growth factor receptor-binding protein-2, and Ras kinase inhibitor-1 [27]. mir-133 inhibits myocardial

Indexed in: [Current Contents/Clinical Medicine] [SCI Expanded] [ISI Alerting System] [ISI Journals Master List] [Index Medicus/MEDLINE] [EMBASE/Excerpta Medica] [Chemical Abstracts/CAS]

fibrosis by reducing the connective tissue growth factor gene and fibrin synthesis [28]. mir-144 analogues transfected into rat H9C2 cardiomyocytes can reduce cell proliferation and increase apoptotic rate by enhancing Caspase-3 activity [29], suggesting its potential utility as a gene promoting cardiomyocyte apoptosis. Studies have reported that mir-378 can inhibit the expression of caspase-3, which can reduce cardiomyocyte ischemic injury, suggesting its utility as a potential therapy target [30].

Regulation of the miRNAs target genes is very important. miRNAs degrade target genes at the post-transcriptional level and inhibit their expression [31]. According to the results of combined analysis of mRNAs and miRNAs, a single miRNAs can regulate multiple target genes, such as mir-3966-x, mir-4510-x, novel-m0002-5p, mir-144-y, and mir-22-y. Bioinformatics analysis showed that a total of 9 miRNAs participated in the construction of the miRNAs-mRNAs regulatory network. These 9 miRNAs had 20 target genes, including FSTL1, LOX, CNN1, ADAMTS8, LTBP2, and other genes closely related to AMI. Studies have shown that myocardial ischemia and hypoxia can induce the expression of FSTL1 and promote compensatory vascular remodeling [32]. Li et al. [33] found that myocardial ischemia/reperfusion injury can increase expression of LOX-1 in the myocardium. The application of an antibody antagonizing LOX-1 function can significantly reduce myocardial injury and infarction size. Wagsater et al. demonstrated enhanced ADAMTS8 expression in carotid atherosclerotic and unstable coronary plaques [34], and Gabrielsen et al. [35] found significantly higher LTBP2 levels in patients with heart failure.

Supplementary Data

Supplementary Table 1. MicroRNA qPCR Primer sequences.

miRNA	Forward primer (5' to 3')
mir-22-y	CCGCTGCCAGTTGAAGAACTGT
mir-495-y	AACAAACATGGTGCACTTCTTT
mir-133-x	AGCTGGTAAAATGGAACCAAATC
mir-144-y	ATACAGTATAGATGATGTACT
mir-136-y	AATCATCGTCTCAAATGAGTCT
mir-3966-x	CAGCTGCCAGTTGCAGAACTGT
U6	CTCGCTTCGGCAGCACA

Conclusions

In this study, we established the expression profiles of DEMs and DEGs in cardiac tissues. A single miRNA can regulate multiple RNAs and a single RNA can be regulated by multiple miRNAs. They interact to form a complex regulatory network and play a role in the development of AMI. The findings of our study provided a basis for the pathogenesis, clinical treatment, and prognosis of CLMN in the treatment of AMI. Our results also provide a theoretical basis for screening the CLMN targets with respect to AMI and provide a platform for the screening of markers.

Acknowledgments

The authors would like to express their gratitude to EditSprings (*https://www.editsprings.com/*) for the expert linguistic services provided.

Conflict of interest

None.

Indexed in: [Current Contents/Clinical Medicine] [SCI Expanded] [ISI Alerting System] [ISI Journals Master List] [Index Medicus/MEDLINE] [EMBASE/Excerpta Medica] [Chemical Abstracts/CAS]

Supplementary Table 2. MRNA qPCR Primer sequences.

Gene	Forward primer	Reverse primer
ENSMUST00000001384 (CNN1)	GGGTTACGGTTTGGGGAGAT	TCAACTCAGTGCTTCCTTCGG
ENSMUST00000163189 (LTBP2)	AGGCTGGGAGTGTGTTGATG	AGTGTCCTTCTTCTGCGTCG
ENSMUST00000001964 (ACE)	GATGGAAGGGAGGTGGTGTG	GTGCGCTATCACCAAGTCCT
ENSMUST00000110347 (SMOC1)	CGACTACTGCGACCTGAACA	GGTTTGTGCCTGCTCGTTTT
ENSMUST00000001534 (SOST)	CCACCCACGGACACATTTCT	TATAACACTTGCGCCCTCCG
ENSMUST00000114763 (FSTL1)	CAATCGCTGTGTCTGTTCCTGT	TGTCTTCTCCTCCTCTGTGTGG
ENSMUST00000171470 (LOX)	TGCCCGACCCCTACTACATCC	TCATAGTCTCTGACATCCGCCC
ENSMUST00000034497 (MMP3)	TTCTGGGCTATACGAGGGCA	CTTCTTCACGGTTGCAGGGA
ENSMUST00000058856 (SCD4)	GCCGTGGCTTCTTCTTCTCT	TCCAGGTTTTTGCCCTTCTC

Supplemenatry Table 3. Results of miRNA sequencing.

Samples	Raw reads	High quality	3'adapter null	Insert null	5'adapter contaminants	Smaller than 18nt	polyA	Clean tags
S-1	1,2E+07	11328752	19137	27173	5684	2E+05	243	10698735
S-2	1,3E+07	12828535	13474	94001	10583	6E+05	326	11656566
S-3	2,3E+07	22087613	31633	155393	16003	6E+05	858	21255112
M-1	2,3E+07	22441987	24642	197003	25177	6E+05	775	21592758
M-2	2,3E+07	22213738	30426	721194	35156	7E+05	417	20666774
M-3	1,3E+07	12178331	12577	55976	11370	3E+05	261	11452776
T-1	1,1E+07	11015425	10337	45158	6720	2E+05	292	10442059
T-2	1,1E+07	10853289	12920	64226	5615	3E+05	132	10169750
T-3	2,4E+07	23193093	26784	452692	28657	2E+06	793	20812146

Supplementary Table 4. The number of Reads in each sample was calculated.

Samples	Number of raw reads	Number of clean reads	The number of reads from the ribosomal database was not matched	The number of reads that were uniquely matched to the reference genome
S-1	6,7E+07	66509234 (98.96%)	66291658 (99.67%)	57055136 (86.07%)
S-2	5,6E+07	54862438 (98.84%)	54730308 (99.76%)	47399155 (86.60%)
S-3	5,9E+07	58432720 (99.03%)	58208154 (99.62%)	50873703 (87.40%)
M-1	6,7E+07	65821074 (98.89%)	65581500 (99.64%)	55991422 (85.38%)
M-2	7E+07	68831828 (98.99%)	68640354 (99.72%)	58598325 (85.37%)
M-3	6,9E+07	68291544 (99.04%)	68144732 (99.79%)	57229687 (83.98%)
T-1	6E+07	59226516 (99.03%)	59100606 (99.79%)	49819176 (84.30%)
T-2	7,2E+07	70798226 (98.98%)	70627160 (99.76%)	59133774 (83.73%)
T-3	6,8E+07	66968094 (98.96%)	66806616 (99.76%)	57421130 (85.95%)

Indexed in: [Current Contents/Clinical Medicine] [SCI Expanded] [ISI Alerting System] [ISI Journals Master List] [Index Medicus/MEDLINE] [EMBASE/Excerpta Medica] [Chemical Abstracts/CAS]

Supplementary Table 5. Gene ontology analyse of differentially expressed mRNAs.

Ontology	Class	Number of up genes	Number of down genes
BP	Developmental process	0	32
BP	Multicellular organismal process	0	35
BP	Biological adhesion	0	10
BP	Biological regulation	0	47
BP	Single-organism process	0	50
BP	Response to stimulus	0	32
BP	Detoxification	0	1
BP	Cell aggregation	0	1
BP	Cellular component organization or biogenesis	0	18
BP	Growth	0	3
BP	Multi-organism process	0	7
BP	Reproductive process	0	5
BP	Reproduction	0	5
BP	Immune system process	0	6
BP	Metabolic process	0	30
BP	Cellular process	0	46
BP	Behavior	0	2
BP	Locomotion	0	3
BP	Localization	0	12
BP	Signaling	0	14
MF	Binding	0	57
MF	Molecular function regulator	0	7
MF	Chemoattractant activity	0	1
MF	Antioxidant activity	0	1
MF	Structural molecule activity	0	3
MF	Catalytic activity	0	19
MF	Transporter activity	0	3
MF	Nucleic acid binding transcription factor activity	0	1
MF	Signal transducer activity	0	3
CC	Extracellular matrix	0	22
CC	Extracellular region	0	48
CC	Extracellular region part	0	43
CC	Extracellular matrix component	0	10
CC	Cell junction	0	3

Indexed in: [Current Contents/Clinical Medicine] [SCI Expanded] [ISI Alerting System] [ISI Journals Master List] [Index Medicus/MEDLINE] [EMBASE/Excerpta Medica] [Chemical Abstracts/CAS]

Supplementary Table 5 continued. Gene ontology analyse of differentially expressed mRNAs.

Ontology	Class	Number of up genes	Number of down genes
CC	Organelle	0	39
CC	Synapse part	0	1
CC	Synapse	0	1
CC	Macromolecular complex	0	12
CC	Membrane-enclosed lumen	0	5
CC	Membrane	0	22
CC	Organelle part	0	13
CC	Cell	0	43
CC	Cell part	0	43
CC	Membrane part	0	12

Supplemnatry Table 6. Pathway of DEGs.

NO	Pathway ID	Pathway	P-value
1	ko04974	Protein digestion and absorption	0.000176
2	ko04510	Focal adhesion	0.004226
3	ko04151	PI3K-Akt signaling pathway	0.025648
4	ko03320	PPAR signaling pathway	0.028982
5	ko04512	ECM-receptor interaction	0.032328
6	ko00590	Arachidonic acid metabolism	0.033014
7	ko04668	TNF signaling pathway	0.047913
8	ko04066	HIF-1 signaling pathway	0.051143
9	ko04614	Renin-angiotensin system	0.060399
10	ko00360	Phenylalanine metabolism	0.072662
11	ko04270	Vascular smooth muscle contraction	0.074852
12	ko04310	Wnt signaling pathway	0.077677
13	ko00340	Histidine metabolism	0.078736
14	ko01040	Biosynthesis of unsaturated fatty acids	0.084772
15	ko00760	Nicotinate and nicotinamide metabolism	0.099696
16	ko00410	beta-Alanine metabolism	0.102653
17	ko00350	Tyrosine metabolism	0.1202
18	ko00591	Linoleic acid metabolism	0.148718
19	ko01212	Fatty acid metabolism	0.1571
20	ko04015	Rap1 signaling pathway	0.171198
21	ko00330	Arginine and proline metabolism	0.176351
22	ko04014	Ras signaling pathway	0.185342
23	ko00980	Metabolism of xenobiotics by cytochrome P450	0.197837

Indexed in: [Current Contents/Clinical Medicine] [SCI Expanded] [ISI Alerting System] [ISI Journals Master List] [Index Medicus/MEDLINE] [EMBASE/Excerpta Medica] [Chemical Abstracts/CAS]

Supplemnatry Table 6 continued. Pathway of DEGs.

NO	Pathway ID	Pathway	P-value
24	ko00982	Drug metabolism-cytochrome P450	0.203125
25	ko00010	Glycolysis/Gluconeogenesis	0.208378
26	ko04060	Cytokine-cytokine receptor interaction	0.207781
27	ko04610	Complement and coagulation cascades	0.226507
28	ko04350	TGF-beta signaling pathway	0.236688
29	ko04916	Melanogenesis	0.285696
30	ko04919	Thyroid hormone signaling pathway	0.327218
31	ko04670	Leukocyte transendothelial migration	0.329456
32	ko04152	AMPK signaling pathway	0.344922
33	ko04611	Platelet activation	0.353606
34	ko04726	Serotonergic synapse	0.35576
35	ko04068	FoxO signaling pathway	0.360046
36	ko04530	Tight junction	0.372744
37	ko04390	Hippo signaling pathway	0.399433
38	ko04921	Oxytocin signaling pathway	0.417271
39	ko04022	cGMP-PKG signaling pathway	0.436495
40	ko04024	cAMP signaling pathway	0.485419
41	ko04810	Regulation of actin cytoskeleton	0.510815
42	ko04080	Neuroactive ligand-receptor interaction	0.665957

Supplementary Table 7. Differential miRNA target genes.
[Supplementary Table 7 available from the corresponding author on request.]

References:

1. Ramón M, Baugh J, Ledwidge M et al: Diastolic heart failure evidence of increased myocardial collagen turnover linked to diastolic dysfunction. Circulation, 2007; 115: 888–95
2. Harvey DW, Derek PC: Acute myocardial infarction. Lancet, 2008; 372: 570–84
3. Dang LJ, Zhang WJ, Liu SY et al: Effect of puerarin in Longmaining formula on pharmacokinetics-pharmacodynamics correlation in rats with myocardial ischemia. China J Chin Mater Med, 2016; 41: 1535–40
4. Corsten MF, Dennert R, Jochems S et al: Circulating microRNA-208b and microRNA-499 reflect myocardial damage in cardiovascular disease. Circ-Cardiovasc Gene, 2010; 3: 499–506
5. Olof Gidlöf, Smith JG, Miyazu K et al: Circulating cardio-enriched microRNAs are associated with long-term prognosis following myocardial infarction. BMC Cardiovasc Disor, 2013; 13: 12
6. Ambros V: The functions of animal microRNAs. Nature, 2004; 431: 350–55
7. Li YS, Xu J, Chen H et al: Comprehensive analysis of the functional microRNA-mRNA regulatory network identifies miRNA signatures associated with glioma malignant progression. Nucleic Acids Res, 2013; 41: e203
8. Monzo M, Navarro A, Bandres E et al: Overlapping expression of microRNAs in human embryonic colon and colorectal cancer. Cell Res, 2008; 18: 823–33
9. Wang CL, Bai XH, Liu SY et al: RNA-seq based transcriptome analysis of the protective effect of compound longmaining decoction on acute myocardial infarction. J Pharmaceut Biomed, 2018; 158: 339–45
10. Lin WL, Lo LW, Chen HR et al: Sleep-related changes in cardiovascular autonomic regulation in left coronary artery ligation rats: Neural mechanism facilitating arrhythmia after myocardial infarction. Int J Cardiol, 2016; 225: 65–72
11. Gouweleeuw L, Hovens IB, Liu H et al: Differences in the association between behavior and neutrophil gelatinase-associated lipocalin in male and female rats after coronary artery ligation. Physiol Behav, 2016; 163: 7–16
12. Simon A, Wolfgang H: Differential expression analysis for sequence count data. Genome Biol, 2010; 11: R106
13. Dalman MR, Deeter A, Nimishakavi G, Duan ZH: Fold change and p-value cutoffs significantly alter microarray interpretations. BMC Bioinformatics, 2012; 13: S11
14. Shunwu Y, Hongyan L, Lijun L: Analysis of relative gene expression using different real-time quantitative PCR. Acta Agronomica Sinica, 2007
15. Zhang XH, Lu ZL, Liu L: Coronary heart disease in China. Heart, 2008; 94: 1126–31

Indexed in: [Current Contents/Clinical Medicine] [SCI Expanded] [ISI Alerting System] [ISI Journals Master List] [Index Medicus/MEDLINE] [EMBASE/Excerpta Medica] [Chemical Abstracts/CAS]

16. Zhuo S: [Experimental study of Fu fang longmaining di wan anti-thrombosis and improving micro-circulation.] J Shaanxi Coll Tradit Chin Med, 2010; 33: 55–57 [in Chinese]
17. Cheng Z, Dimichele LA, Hakim ZS et al: Targeted focal adhesion kinase activation in cardiomyocytes protects the heart from ischemia/reperfusion injury. Arterioscler Thromb Vasc Biol, 2012; 32: 924–33
18. Xu L, Jiang X, Wei F, Zhu HL: Leonurine protects cardiac function following acute myocardial infarction through anti-apoptosis by the PI3K/AKT/GSK3β signaling pathway. Mol Med Rep, 2018; 18: 1582–90
19. Morrison A, Li J: PPAR-γ and AMPK – advantageous targets for myocardial ischemia/reperfusion therapy. Biochem Pharmacol, 2011; 82: 195–200
20. Li YY, McTieman CF, Feldman AM: Interplay of matrix metalloproteinases tissue inhibitors of metalloproteinases and their regulators in cardiac matrix remodeling. Cardiovasc Res, 2000; 46: 214–24
21. Passino C, Barison A, Vergaro G et al: Markers of fibrosis, inflammation, and remodeling pathways in heart failure. Clin Chim Acta, 2015; 443: 29–38
22. Dohn TE, Waxman JS: Distinct phases of Wnt/beta-catenin signaling direct cardiomyocyte formation in zebrafish. Dev Biol, 2012; 361: 364–76
23. Du JK, Cong BH, Yu Q et al: Upregulation of microRNA-22 contributes to myocardial ischemia-reperfusion injury by interfering with the mitochondrial function. Free Radical Bio Med, 2016; 96: 406–17
24. Gurha P, Wang T, Larimore AH et al: MicroRNA-22 promotes heart failure through coordinate suppression of PPAR/ERR-nuclear hormone receptor transcription. PLoS One, 2013; 8: e75882
25. Gurha P, Abreugoodger C, Wang T et al: Targeted deletion of microRNA-22 promotes stress-induced cardiac dilation and contractile dysfunction. Circulation, 2012; 125: 2751–61
26. Hong Y, Cao H, Wang Q et al: MiR-22 may suppress fibrogenesis by targeting TGFβR I in cardiac fibroblasts. Cell Physiol Biochem, 2016; 40: 1345–53
27. Ganesan J, Ramanujam D, Sassi Y et al: MiR-378 controls cardiac hypertrophy by combined repression of mitogen-activated protein kinase pathway factors. Circulation, 2013; 127: 2097–106
28. Duisters RF, Tijsen AJ, Schroen B et al: miR-133 and miR-30 regulate connective tissue growth factor implications for a role of MicroRNAs in myocardial matrix remodeling. Circ Res, 2009; 104: 170–78
29. Huang F, Huang XY, Yan DS et al: MicroRNA-144 over-expression induced myocytes apoptosis. Zhonghua Xin Xue Guan Bing Za Zhi, 2011; 39: 353–57
30. Fang J, Song XW, Tian J et al: Overexpression of microRNA-378 attenuates ischemia-induced apoptosis by inhibiting caspase-3 expression in cardiac myocytes. Apoptosis, 2012; 17: 410–23
31. Lau NC, Lim LP, Weinstein EG, Bartel DP: An abundant class of tiny RNAs with probable regulatory roles in *Caenorhabditis elegans*. Science, 2001; 294: 858–62
32. Ouchi N, Oshima Y, Ohashi K et al: Follistatin-like 1, a secreted muscle protein, promotes endothelial cell function and revascularization in ischemic tissue through a nitric-oxide synthase-dependent mechanism. J Biol Chem, 2008; 283: 32802–11
33. Li D, Williams V, Liu L et al: Lox-1 inhibition in myocardial ischemia-reperfusion injury: Modulation of mmp-1 and inflammation. Am J Physiol Heart Circ Physiol, 2002;283: 1795–801
34. Wagsater D, Bjork H, Zhu C et al: Adamts-4 and Adamts-8 are inflammatory regulated enzymes expressed in macrophage-rich areas of human atherosclerotic plaques. Atherosclerosis, 2008; 196: 514–22
35. Gabrielsen A, Lawler PR, Yongzhong W et al: Gene expression signals involved in ischemic injury, extracellular matrix composition and fibrosis defined by global mRNA profiling of the human left ventricular myocardium. J Mol Cell Cardiol, 2007; 42: 870–83

Indexed in: [Current Contents/Clinical Medicine] [SCI Expanded] [ISI Alerting System] [ISI Journals Master List] [Index Medicus/MEDLINE] [EMBASE/Excerpta Medica] [Chemical Abstracts/CAS]